

Constrained randomisation of weighted networks

Gerrit Ansmann* and Klaus Lehnertz†

*Department of Epileptology, University of Bonn,
Sigmund-Freud-Straße 25, 53105 Bonn, Germany*

*Helmholtz Institute for Radiation and Nuclear Physics, University of Bonn,
Nussallee 14–16, 53115 Bonn, Germany and*

*Interdisciplinary Center for Complex Systems, University of Bonn,
Brühler Straße 7, 53175 Bonn, Germany*

We propose a Markov chain method to efficiently generate *surrogate networks* that are random under the constraint of given vertex strengths. With these strength-preserving surrogates and with edge-weight-preserving surrogates we investigate the clustering coefficient and the average shortest path length of functional networks of the human brain as well as of the International Trade Networks. We demonstrate that surrogate networks can provide additional information about network-specific characteristics and thus help interpreting empirical weighted networks.

PACS numbers: 89.75.Hc, 87.19.lj, 05.45.Tp, 02.70.Uu, 89.75.-k

I. INTRODUCTION

Over the past decade, network theory has contributed significantly to improve our understanding of collective dynamics in networks with complex topologies. The simplicity of the network representation, where the interactions and interacting elements are mapped to edges and vertices, respectively, stimulated its use on a number of systems, ranging from physical, biological to social and engineering systems [1–12]. A large number of natural and man-made systems have been shown to be neither entirely regular nor entirely random, but to exhibit prominent topological properties, such as short average path lengths and a high level of clustering.

Recently, weighted networks, in which each edge is assigned a weight, have been shown to allow a better description of many natural and man-made systems [4, 8, 13–17], and particularly of functional networks underlying various brain pathologies [18–23]. Functional brain networks are usually derived from either direct or indirect measurements of neural activity. Network vertices are associated with sensors that are placed such as to sufficiently capture the dynamics of different brain regions. The connectedness between any pair of brain regions is assessed by evaluating some linear or non-linear interdependencies between their neural activities [24–27]. Such networks can be regarded as complete weighted networks, in which all possible edges exist.

For empirical networks, interpreting findings is not without challenges. Findings of some network characteristics may be influenced by statistical fluctuations (like measurement or environmental noise) and systematic errors (which might, for example, be attributed to the data acquisition or to the selected way to construct a network from the data). Moreover, existing methods of analysis

may be misapplied or misinterpreted, which may lead to inappropriate conclusions, as pointed out in Refs. [28–30]. Standard approaches to uncovering influencing factors like background measurements, repeated measurements, or selective manipulation of the investigated system may, however, not be feasible in empirical network studies. Another strategy is the comparison with the expected result for appropriate null models. This result can either be derived analytically [31–33] or be extracted from samples that are obtained by Monte Carlo simulations [14, 34–42]. In the following we refer to these samples as ‘surrogate networks’, in accordance with a similar approach, that is well established in time series analysis [43, 44].

We here propose an efficient iterative procedure to generate strength-preserving surrogate networks for investigations of complete weighted networks. This paper is organised as follows. In Sec. II we describe our approach to surrogate networks and introduce our procedure. We show that it generates approximately uniformly distributed surrogates for a sufficient number of iterations and propose a method to determine this number. With strength-preserving surrogates and weight-preserving surrogates we reanalyse functional networks of the human brain and investigate the International Trade Networks (Sec. III). We demonstrate that surrogates can provide additional information about network-specific characteristics and thus aid in their interpretation. Finally, in Sec. IV we draw our conclusions.

II. METHODS

A. Definitions and Measures

We consider undirected, weighted networks with non-negative edge weights and treat them as complete networks, i.e., we consider every possible edge to exist. A network of this type with n vertices is fully described by its symmetric non-negative weight matrix $W \in \mathbb{R}_+^{n \times n}$, whose entry W_{ij} is the weight of the edge connecting ver-

* gansmann@uni-bonn.de

† klaus.lehnertz@ukb.uni-bonn.de

tices i and j . For practical purposes we define the diagonal elements W_{ii} as zero. The strength of a vertex is defined as the sum of all adjacent weights $S_i := \sum_{j=1}^n W_{ij}$. We consider the distribution of all edge weights of a network $\mathcal{W} := \{W_{12}, W_{13}, W_{23}, \dots, W_{n-1,n}\}$ and the distribution of all vertex strengths $\mathcal{S} := \{S_1, \dots, S_n\}$.

For the weighted clustering coefficient of node i we use the following definition [45]:

$$C_i := \frac{\sum_{jk} \sqrt[3]{W_{ij}W_{jk}W_{ki}}}{(n-1)(n-2) \max(\mathcal{W})}.$$

This definition has the advantage that the value of the clustering coefficient is continuous for $W_{ij} \rightarrow 0$ [46]. We also consider

$$K_i := \frac{\sum_{jk} \sqrt[3]{W_{ij}W_{jk}W_{ki}}}{(n-1)(n-2)} = C_i \max(\mathcal{W}).$$

For the weighted shortest path L_{ij} between vertices i and j we follow Ref. [47] and consider the inverse of the weight of an edge as the length of that edge.

As network specific characteristics we here investigate the averages \bar{C} , \bar{K} , and \bar{L} of C_i , K_i , and L_{ij} , respectively.

B. Network Surrogates

We consider the extent, to which distributions of local network properties (such as \mathcal{W} or \mathcal{S}) contribute to the network-specific characteristic under investigation (such as \bar{C} , \bar{K} , or \bar{L}). In many situations this quantity may reveal important aspects of the network or of the applied methods:

- If the edge weights—instead of being determined by the investigated system—are independently drawn from some distribution (e.g., due to excessive noise), the value of any characteristic can only be attributed to the weight distribution \mathcal{W} and to coincidence.
- Edge weights defined from the data are often normalised by multiplication with a factor, that depends on a distribution of local properties (e.g., the average strength \bar{S}). This usually changes the extent, to which this distribution contributes to network-specific characteristics. Sign and magnitude of this change may help to decide, whether a normalisation works as intended.
- If the weight of an edge only depends monotonically on some intrinsic property of its adjacent vertices (e.g., in fitness model networks [48, 49]), the value of network-specific characteristics may be mainly attributed to the strength distribution \mathcal{S} .
- If one local entity (e.g., an edge weight) dramatically exceeds the others in some local property (e.g.,

if the maximum edge weight is by far larger than the other weights), it may dominate a network-specific characteristic. As this influence is mediated by the distribution of this property, the network-specific characteristic would be mainly attributed to this distribution.

- If the value of a network-specific characteristic can be fully attributed to the distribution of a local network property, it should be considered, whether in this case a network approach to the data is overly complicated and more simple properties may be regarded instead.

To decide, to which extent a characteristic of a given network (the ‘original network’) is determined by the distribution of a local network property, it can be compared to the values for surrogates of this network, which are randomised under the constraint that this distribution is preserved. Moreover, the null hypothesis can be tested, that the network under consideration is random under the constraint of the distribution of the local property. Details about null hypothesis tests based on surrogates can be found in the literature, e.g., in Ref. [44].

We here consider surrogate methods, which exactly preserve either the strength distribution \mathcal{S} or the weight distribution \mathcal{W} (preserving both would in most cases only leave one possible surrogate network, namely, the original network). We aim at methods that sample uniformly from the set of all networks with a given \mathcal{S} or \mathcal{W} , respectively. The corresponding null hypotheses are

$H_{\mathcal{S}}$: The network under consideration is random under the constraint of its strength distribution \mathcal{S} .

$H_{\mathcal{W}}$: The network under consideration is random under the constraint of its weight distribution \mathcal{W} .

Note that preserving the strength distribution is equivalent to preserving the strength sequence when regarding network-specific properties, since they are not affected by a permutation of the vertices. While the generation of uniformly-distributed weight-preserving surrogates can be achieved by a reshuffling of the weights [14, 40], our method to generate strength-preserving surrogates is described in the following.

C. Strength-preserving surrogate networks

The constraint of a given strength sequence of an undirected, weighted, and complete network with n vertices can be expressed by a system of n linear equations with the $m := \frac{1}{2}n(n-1)$ edge weights as variables. Given the non-negativity of the edge weights the set of solutions to this set of equations represents a convex polytope $\Omega \in \mathbb{R}^m$ [50], each point of which corresponds to a network. Thus the problem of generating strength-preserving surrogates is equivalent to that of picking random points from a polytope. Some exact solutions to

this problem (e.g., utilizing triangulation) have been proposed [51], but due to computational burden they may be applied to networks with a very small number of vertices only. Hit-and-Run samplers [52] are a group of iterative Monte-Carlo procedures providing samples from a bounded region, such as a polytope. The distribution of these samples has been shown to approximate the uniform distribution on that region under certain requirements and for a sufficient number of iterations [53]. We here propose a Hit-and-Run sampler, that is specialised to the problem of generating strength-preserving surrogates. In Appendix A we present a mathematical background to this procedure and show, that it fulfils the requirements for sampling approximately uniform.

1. Procedure

We propose the following procedure for sampling from the set Ω of all networks with a given strength sequence:

1. Acquire some network $P^0 \in \Omega$ and set the counter $h = 1$.
2. Randomly select four pairwise distinct vertex indices $i, j, k, l \in \{1, \dots, n\}$.
3. Pick a number ζ from the uniform distribution on $\left[-\min(P_{ij}^{h-1}, P_{kl}^{h-1}), \min(P_{jk}^{h-1}, P_{li}^{h-1})\right]$. Let $P^h = P^{h-1}$, but set $P_{ij}^h = P_{ij}^{h-1} + \zeta$, $P_{jk}^h = P_{jk}^{h-1} - \zeta$, and $P_{kl}^h = P_{kl}^{h-1} + \zeta$, $P_{li}^h = P_{li}^{h-1} - \zeta$ (cf. Fig. 1).
4. If $h < t$, raise h by 1 and continue at 2. Otherwise let P^t be the surrogate network.

The interval, to which ζ is limited, is the maximum one, such that the transformed network does not contain any negative weights. This procedure can be regarded as an extension of previously suggested null model samplers [34, 35, 39, 41].

In principle, P^t as generated by our procedure is statistically dependent on P^0 . This dependence becomes negligible, however, for a sufficiently high number of transformations t_{suf} (to be determined in Sec. II C 2). Most computational effort has to be spent reducing this statistical dependence.

Concerning the acquisition of the starting point P^0 , the most direct approach would be to select $P_i^0 = O \forall i$, where O is the original network and the subscript index here indicates different surrogates to be generated. This way, however, the reduction of statistical dependence achieved when generating surrogate P_{i-1}^t is discarded when generating surrogate P_i^t . To benefit more from previously achieved reductions of dependence, we therefore employed schemes, where P_i^0 is a previously generated surrogate for most i (e.g., $P_i^0 = P_{i-1}^t$). Out of several such schemes, the one depicted in Fig. 2 required the smallest number of total iterations to generate 4096

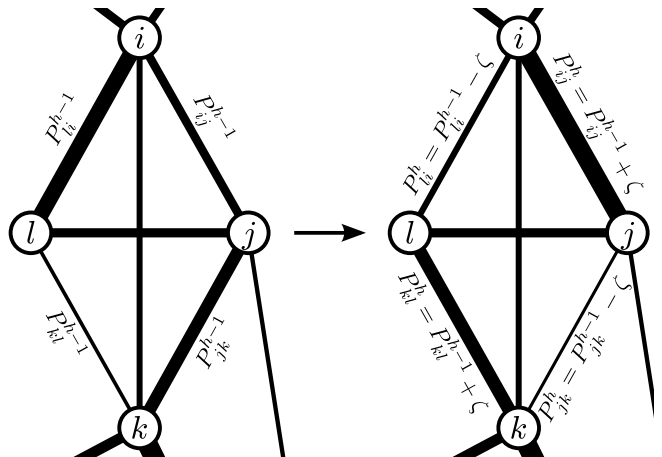


FIG. 1. ‘Tetragon transformation’ of the network P^{h-1} to P^h . In a randomly selected tetragon (i, j, k, l) a random number ζ is added to the weights of two opposing edges $(P_{ij}^{h-1}, P_{kl}^{h-1})$ and subtracted from the weights of the others $(P_{jk}^{h-1}, P_{li}^{h-1})$. Other edge weights remain unaltered. Edge weights are encoded as line thickness.

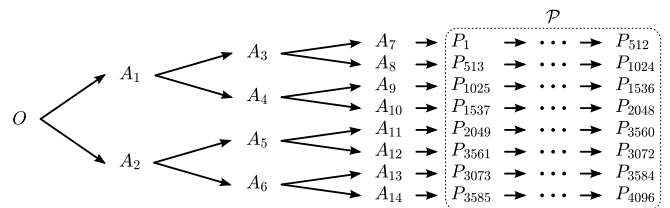


FIG. 2. Scheme used to generate surrogates $\mathcal{P} = \{P_1, \dots, P_{4096}\}$ from an original network O . Short arrows represent a ‘step’ consisting of t tetragon transformations, long arrows represent ten such steps, A_1, \dots, A_{14} are auxiliary networks. (Superscripts are omitted for better readability.)

surrogates with negligible dependencies (according to the test presented in Sec. II C 2). This scheme was roughly ten times faster than the direct generation of surrogates from the original network ($P_i^0 = O$).

2. Numerical estimation of the necessary number of transformations

In order to estimate, which number t of transformations is sufficient, we employed the following procedure to test whether surrogate networks are sampled appropriately. It estimates the likelihood that surrogates $\mathcal{P} = \{P_1, \dots, P_a\}$ ($a \in \mathbb{N}$) are picked independently from the uniform distribution.

1. Select parameters $b, c \in \mathbb{N}$ with $c \ll a$.
2. Generate a surrogates $\mathcal{Q} = \{Q_1, \dots, Q_a\}$ with a ‘reference method’ that is known to pick surrogates independently from the uniform distribution. Pick some random testing points $\mathcal{R} = \{R_1, \dots, R_b\}$ from the polytope Ω , e.g., by using the reference method.

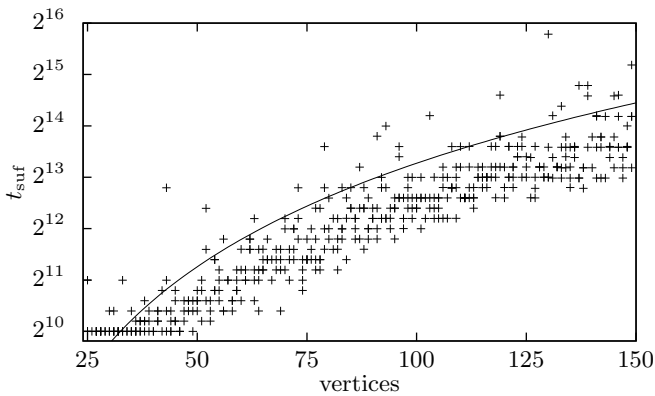


FIG. 3. Number of sufficient transformations t_{suf} per step for the generation of 4096 surrogate networks from four toy networks with n vertices. For comparison, the solid line displays twice the number of edges.

3. For all $i \in \{1, \dots, b\}$, determine $\epsilon_i > 0$ such that exactly c surrogates from \mathcal{Q} are in the ϵ_i -ball around R_i .
4. For all $i \in \{1, \dots, b\}$, let k_i be the number of surrogates from \mathcal{P} in the ϵ_i -ball around R_i .

5. Let $\tilde{p}(k) := \binom{a}{k} \binom{2a}{c+k}^{-1}$ and $\chi := \frac{1}{b} \left(\sum_{i=1}^b \tilde{p}(k_i) \right) \left(\sum_{j=0}^a \tilde{p}(j) \right) \left(\sum_{j=0}^a \tilde{p}(j)^2 \right)^{-1}$. The expected value of χ is 1 if P_1, \dots, P_a are picked independently from the uniform distribution. Otherwise and if a and b are sufficiently high and c is sufficiently low, the expected value of χ is lower than 1 (cf. App. B for details).

To estimate the necessary number t of transformations per step (cf. Fig. 2), we regarded four toy networks with random weights for each number of vertices between 25 and 149. We raised t from 1024 successively by a factor of $2^{0.2}$. For each t we generated several realisations \mathcal{P} of 4096 surrogates each and if $\chi > 0.96$ for each \mathcal{P} , we set $t_{\text{suf}} = t$. As a reference method we used the same method with $t = 2^{19}$, which we assumed to generate appropriately sampled surrogates. To avoid the reference \mathcal{Q} being statistically outlying, however, we omitted it, if it scored $\chi < 0.98$ in a test against another reference generated by the same method. For comparison, $\chi = 1.01 \pm 0.03$ for the reference methods in a test against themselves. In Fig. 3 we show the number of sufficient transformations t_{suf} for different numbers of vertices of the toy networks. We observe that in most cases our method generates appropriate surrogates if t is approximately twice the number of edges in the original network.

Generating 4096 surrogate networks with $t = 2^{16}$ transformations per step took 123s on a PC with 829 MFLOPS (2 GHz).

III. SURROGATE ANALYSIS OF EMPIRICAL NETWORKS

A. Functional brain networks

Characterizing anatomical and functional connections in the human brain with approaches from network theory has been a rapidly evolving field recently [7–9]. Research over the past years indicates that both physiological and pathophysiological states of the brain are reflected by topological aspects of functional brain networks. Mostly the clustering coefficient, the average shortest path length or similar measures had been used to characterise these networks. Findings that had been achieved so far can be regarded as important since they provide new insights into properties of normal and pathological functional brain networks.

In Ref. [22] functional brain networks derived from electroencephalographic (EEG) recordings during different states of vigilance (eyes opened and eyes closed) of 21 epilepsy patients and of 23 healthy control subjects had been analysed using the clustering coefficient \bar{C} and the average shortest path length \bar{L} . Differences in these characteristics could be observed between epilepsy patients and healthy control subjects as well as between states of vigilance. We here reanalysis exemplary networks from an epilepsy patient and a healthy control subject, and with surrogate networks we investigated to which extent the observed findings can be attributed to the weight distribution \mathcal{W} or strength distribution \mathcal{S} .

Details of the data and of recording and analysis techniques are fully described in Ref. [22]. Briefly, EEG data had been recorded for 30 min with $n = 29$ electrodes [54] placed according to the 10-10 system of the American Electroencephalographic Society with the right mastoid as physical reference (sampling rate: 254.31 Hz; 16 bit A/D conversion; bandwidth: 0–50 Hz). During one half of the recording time each subjects had their eyes opened or closed, respectively.

EEG signals were split into consecutive non-overlapping segments of 4096 data points (16.1 s) each. For each segment we extracted the phases in a frequency-selective way using Morlet wavelets centred in the so-called alpha band (8–13 Hz) [55] and calculated the mean phase coherence R_{ij} [56] as a measure for interdependence between signals recorded at sensors i and j (for simplicity's sake we omit the dependence on the segment in the following). R_{ij} is confined to the interval $[0, 1]$ where $R_{ij} = 1$ indicates fully synchronised systems. Network vertices were identified with sensors and edges between vertices i and j were assigned the weight $W_{ij} = R_{ij} - \bar{R} + 1$, where \bar{R} is the average over all R_{kl} with $k \neq l$. For each of these networks, we generated 4096 weight-preserving surrogates and 4096 strength-preserving surrogates and calculated the clustering coefficients \bar{C} and \bar{K} as well as the average shortest path length \bar{L} for the original and the surrogate networks. Note, that for many applications, such as a test of a null hypothesis,

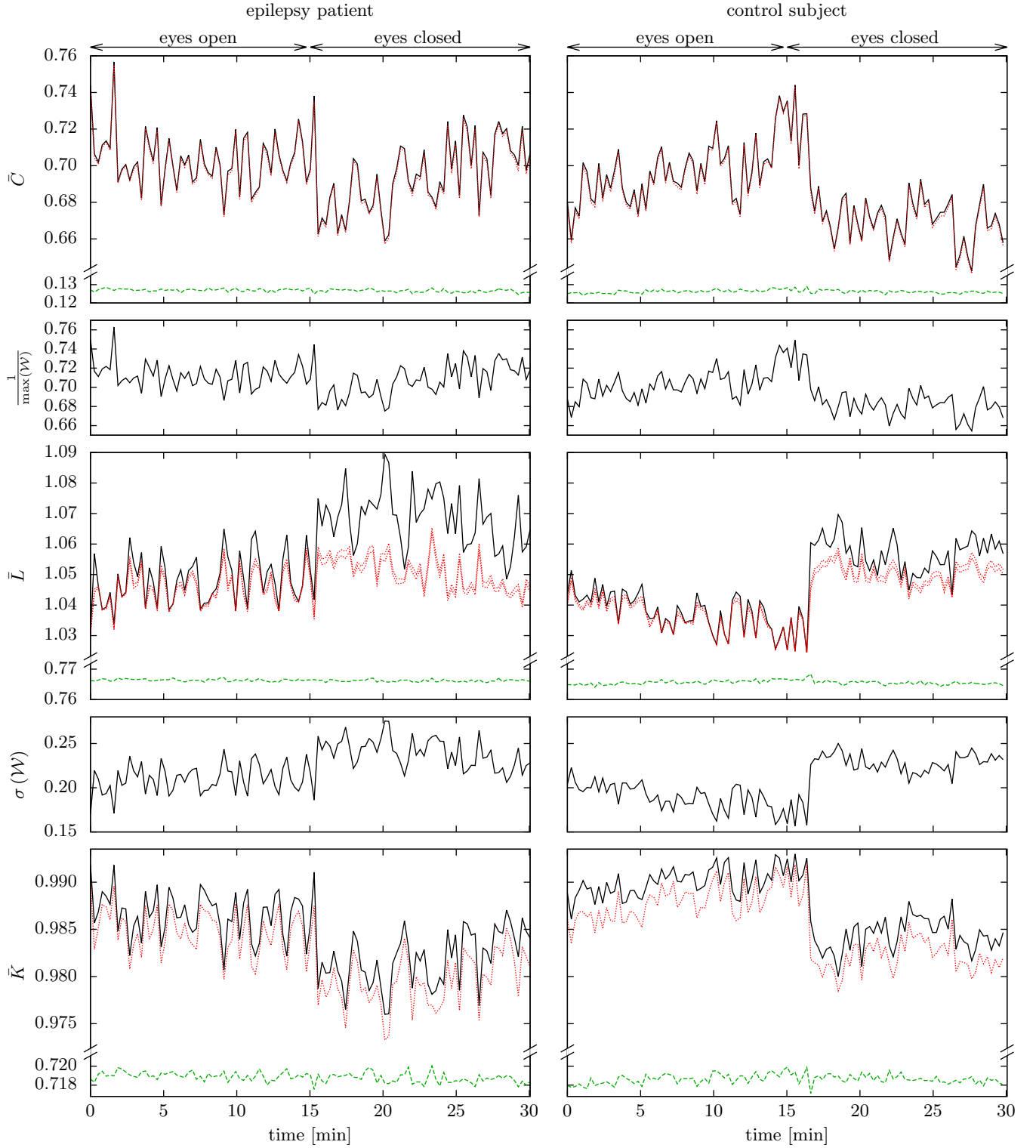


FIG. 4. Temporal evolutions of clustering coefficients \bar{C} (first row) and \bar{K} (fifth row) and average shortest path length \bar{L} (third row) of functional brain networks (black solid lines) and of weight-preserving surrogates (red dotted lines) and strength-preserving surrogates (green dashed lines) for these networks. For \bar{L} we show the margins of standard deviation over 4096 weight-preserving surrogates (red dotted lines). Standard deviations of \bar{C} and \bar{K} over the weight-preserving surrogates were too small to be displayed, the maximum standard deviation of \bar{C} , \bar{K} , and \bar{L} over the 4096 strength-preserving surrogates was 0.02 each. For comparison, for the original networks we show the temporal evolutions of the inverse of the maximum weight $\frac{1}{\max(\mathcal{W})}$ (second row) and of the standard deviation $\sigma(\mathcal{W})$ of the edge weights (fourth row).

fewer surrogates may suffice [44].

In Fig. 4 we show the temporal evolutions of \bar{C} , \bar{K} , and \bar{L} for the functional networks of the epilepsy patient and the healthy control subject and for the corresponding weight- and the strength-preserving surrogates. For both subjects we observed, on average, higher values of \bar{L} and lower values of \bar{C} and \bar{K} during the eyes-closed condition. There were, however, no clear-cut differences in \bar{C} , \bar{K} , and \bar{L} between the epilepsy patient and the control subject. \bar{L} during the eyes-open condition as well as \bar{C} and \bar{K} during the complete observation time were approximately equal for the original networks and the weight-preserving surrogates. A property of the weight distribution \mathcal{W} , that we could identify as strongly correlated to \bar{C} , was the inverse of the maximum edge weight $\frac{1}{\max(\mathcal{W})}$. We attribute this strong influence of $\max(\mathcal{W})$ mainly to its utilisation as a normalisation factor when calculating \bar{C} , since \bar{K} did not exhibit such a strong correlation to $\frac{1}{\max(\mathcal{W})}$. The temporal evolution of \bar{L} was similar to that of the standard deviation of the edge weights of the original network $\sigma(\mathcal{W})$, while the temporal evolution of \bar{K} was opposite to that of $\sigma(\mathcal{W})$.

Despite the mostly similar temporal evolutions of \bar{C} , \bar{K} , and \bar{L} for the original and the weight-preserving surrogate networks, these characteristics always assumed higher values for the original networks than for any of the 4096 surrogates. Thus we can reject the null hypotheses $H_{\mathcal{W}}$, that the original networks are random under the constraint of their weight distribution \mathcal{W} .

When compared to the strength-preserving surrogates \bar{C} , \bar{K} , and \bar{L} always assumed clearly higher values for the original networks, and we could not observe comparable temporal evolutions. The null hypotheses $H_{\mathcal{S}}$, that the original networks are random under the constraint of their strength distribution \mathcal{S} , can be rejected as well.

Our findings indicate that the clustering coefficient \bar{C} of the functional brain networks investigated here is predominantly determined by properties of the weight distribution \mathcal{W} . Similar conclusions can be drawn for the clustering coefficient \bar{K} and the average shortest path length \bar{L} , for the latter, however, for the eyes-open condition only. In contrast, the clear differences between original and surrogate networks seen for \bar{L} during the eyes-closed condition indicate that a considerable part of the value of this network-specific characteristic is not determined by the weight distribution \mathcal{W} of the functional brain networks. Whether these findings hold for all the data investigated in Ref. [22] needs further investigations, which will be published elsewhere.

B. International Trade Networks

As a second example we investigated the clustering coefficients \bar{C} and \bar{K} as well as the average shortest path length \bar{L} of the International Trade Networks (ITN) [46, 57–61] for the years 1948 to 2000. The vertices of the ITNs are countries and the edge weights represent the

amount of trade between the corresponding countries. The number of vertices n of the ITNs changes annually, growing from $n = 73$ in 1948 to $n = 187$ in 2000. Since some binary properties of ITN of 1995 could be explained by a fitness model [58], it is conceivable that the structure of a weighted ITN is also governed by vertex-intrinsic parameters, which are reflected by the countries' total trade activity. Since the latter corresponds to the vertex strengths, strength-preserving surrogates might detect such an influence. As the number of vertices n is preserved alongside with the strength distribution \mathcal{S} and with the weight distribution \mathcal{W} , respectively, strength- or weight-preserving surrogates might help to detect a possible influence of this number on the network-specific characteristics.

To construct the networks from the data we followed Refs. [46, 61] to determine the trade flow between two countries i and j :

$$F_{ij} = \frac{1}{2} (E_{ij} + I_{ij} + E_{ji} + I_{ji})$$

where E_{ij} and I_{ij} denote the export and import from country i to country j . We determined the weights as $W_{ij} = F_{ij}/\bar{F}$, where \bar{F} is the average over all F_{ij} with $i \neq j$. In each year we omitted countries, of which no trade was recorded at all [62]. 47% of the edges of these networks were zero-weight edges. 47% of this zero-weight edges were in turn to be attributed to missing data. The latter (and probably some of the other zero-weight edges) are likely to correspond to small or negligible trade [57]. For each year we calculated \bar{C} , \bar{K} , and \bar{L} of the ITNs as well as of 4096 weight-preserving surrogates and strength-preserving surrogates each.

In the top row of Fig. 5 we show the temporal evolutions of \bar{K} and \bar{L} for the ITNs and for the weight-preserving surrogates and strength-preserving surrogates. For most years both characteristics of the ITNs clearly deviated from the respective values of the surrogates, and we thus can reject the null hypotheses $H_{\mathcal{W}}$ and $H_{\mathcal{S}}$, that the ITNs are random under the constraint of their weight distribution \mathcal{W} or strength distribution \mathcal{S} , respectively.

We observed, however, considerable similarities in the temporal evolutions of \bar{L} for the ITNs and for the strength-preserving surrogates, which approximately differed by a constant factor only (note, that the curves are almost parallel in the semi-logarithmic plot). Hence it should be considered that the temporal changes of \bar{L} can mainly be attributed to changes of \mathcal{S} (i.e., of the annual relative trade volumes and the number of countries), though the absolute value of \bar{L} cannot be attributed to them. The similarities of the temporal evolutions of \bar{K} between the ITNs and the surrogates are less dominant, but apparent for both types of surrogates. This indicates that the temporal changes of \bar{K} can only partially be attributed to changes of \mathcal{W} or \mathcal{S} . In the bottom right part of Fig. 5 we show the temporal evolution of $1/n$, which we observe to be similar to that of \bar{K} . Increases of the number n of countries, however, mostly coincide with sep-

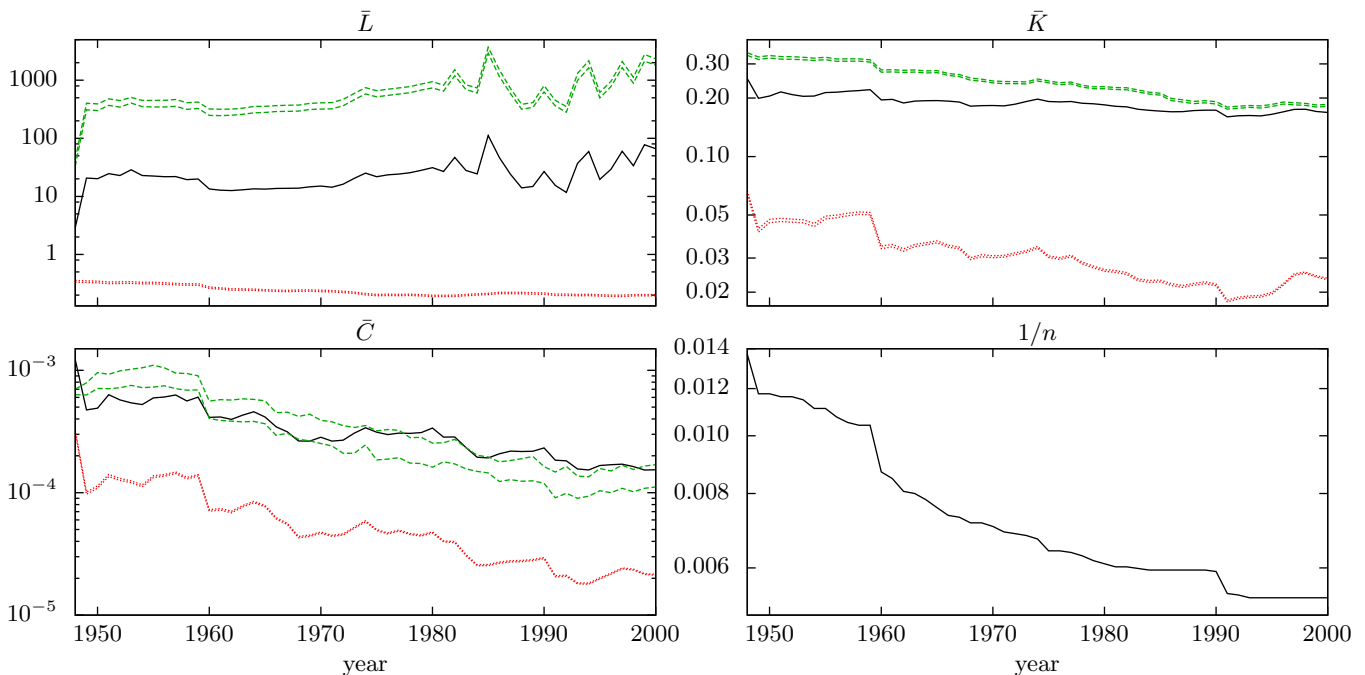


FIG. 5. Top: temporal evolutions of clustering coefficient \bar{K} (right) and average shortest path length \bar{L} (left) of the International Trade Networks for the years 1948 to 2000 (black solid lines). Also shown are the margins of standard deviation for 4.096 weight-preserving surrogates (red dotted lines) and 4.096 strength-preserving surrogates (green dashed lines) for these networks. Bottom left: the same for the clustering coefficient \bar{C} . Bottom right: the inverse of the number of vertices $\frac{1}{n}$ for comparison.

arations of countries, which in turn may also affect \mathcal{W} or \mathcal{S} . Thus our findings do not resolve whether there is a direct influence of n on \bar{K} . The similarities of the temporal evolutions of \bar{K} and \bar{L} between the original networks and the surrogates indicate that there are only few changes in properties not to be attributed to the strength or weight distribution, respectively, and thus affirm that the ITNs' structure is mainly time-invariant [60, 61].

In the bottom left part of Fig. 5 we show the temporal evolutions of \bar{C} for the ITNs and for the weight-preserving surrogates and strength-preserving surrogates. We observe strong similarities in the temporal evolutions of \bar{C} for the ITNs and the weight-preserving surrogates as well as of $\frac{1}{\max(\mathcal{W})}$ (not shown here). These similarities and the fact that they are less pronounced for \bar{K} affirm our findings in Sec. III A that $\max(\mathcal{W})$ strongly influences \bar{C} due to its use as a normalisation constant.

IV. CONCLUSIONS

We proposed a method to efficiently generate strength-preserving surrogates for complete weighted networks. With strength-preserving surrogate networks and weight-preserving surrogate networks we reanalysis functional brain networks and investigated the International Trade Networks. While we were exemplarily regarding the clustering coefficient and the average shortest path length, surrogate networks can also be applied to investigate

other network-specific characteristics.

For functional brain networks derived from an epilepsy patient and a healthy control subject during different states of vigilance we observed that the clustering coefficients \bar{C} and \bar{K} as well as the average shortest path length \bar{L} are strongly dominated by properties of the weight distribution \mathcal{W} , namely, its standard deviation and its maximum. Thus, previously reported differences between subjects as well as between states may be more easily identifiable by merely analysing properties of the distribution of interaction strengths \mathcal{W} . Also, given the strong dependence of the clustering coefficient \bar{C} on the maximum weight, other normalisations for \bar{C} may be more appropriate for a comparison of networks. It is even conceivable that, if the respective maximum weight of the networks under comparison is always held by the same edge, a comparison of the weights of this single edge suffices to identify differences. In such a case a network approach to the data is questionable, since it is an overly complicated description of a simple aspect of the data.

For the International Trade Networks we observed that relative changes of the average shortest path length over the period 1948 to 2000 were reflected by the strength-preserving surrogates. Similar results could also be obtained for the clustering coefficient \bar{K} , whose temporal evolution was also similar to that of the number of vertices. This led us to assume that the relative changes were reflecting alterations of the vertex strengths, which are proportional to the trade volumes of the respective

they may be used as direction set \mathcal{D} for the Hit-and-Run-Sampler. Otherwise or if in doubt, it can still be resorted to a Hypersphere Directions Hit-and-Run Sampler. In the following we provide two examples, how further constraints can be incorporated into the Hit-and-Run sampler framework:

- The constraint that the weights of the surrogates may not exceed a given maximum can be regarded analogously to the constraint of non-negative edge-weights. The set of possible surrogates is a smaller $(m - n)$ -polytope with Λ as affine hull. Thus tetragon transformations can still transform all points of the relative interior of the new polytope into each other. App. A 2 b can be analogously applied to the constraint of a maximum weight. Problems may arise only in the case of zero-weight and maximum-weight edges in the same network.
- If the binary structure of the original network is to be preserved, zero-weight edges remain unaltered and the set of possible surrogates is a bounding sub-polytope of Ω . For sparse networks, however, the requirement of accessibility of all points with tetragon transformations may not be fulfilled.

Appendix B: Properties of the test statistics χ

If points $\mathcal{Q} = Q_1, \dots, Q_a$ ($a \in \mathbb{N}$) are picked independently from the uniform distribution on Ω , the probability π that c of them are in a given ϵ -ball (or any other subset of Ω) is binomially distributed:

$$\pi = B(c, \varrho, a) \equiv \binom{a}{c} \varrho^c (1 - \varrho)^{a-c},$$

$\varrho \in [0, 1]$ being the fraction of Ω 's volume that is occupied by the ϵ -ball. If a priori all ϱ are equiprobable, the probability density of a given ϱ is proportional to π .

If now P_1, \dots, P_a are also picked independently from the uniform distribution, the probability $p(k)$ that k of them are in the same ϵ -ball is proportional to

$$\int_0^1 B(c, \varrho, a) B(k, \varrho, a) d\varrho =: \hat{p}(k).$$

Multiple integrations by parts yield

$$\hat{p}(k) = \frac{1}{2a+1} \binom{a}{c} \binom{a}{k} \binom{2a}{c+k}^{-1}$$

and normalisation finally results in

$$p(k) = \hat{p}(k) \left(\sum_{i=0}^a \hat{p}(i) \right)^{-1} = \tilde{p}(k) \left(\sum_{i=0}^a \tilde{p}(i) \right)^{-1},$$

with $\tilde{p}(k) := \binom{a}{k} \binom{2a}{c+k}^{-1}$.

For the calculation of χ several ϵ_i -balls ($i \in \{0, \dots, b\}$, $b \in \mathbb{N}$) around randomly picked points R_1, \dots, R_b are regarded, each containing exactly c points from \mathcal{Q} . The points $\mathcal{P} = P_1, \dots, P_a$ were picked independently from an unknown distribution, and k_i points from \mathcal{P} are in the ϵ_i -ball around R_i . In this case, the higher $\hat{\chi} := \sum_{i=1}^b p(k_i)$ the more likely it is, that the points \mathcal{P} are picked from the uniform distribution on Ω . Moreover, for $a, b \rightarrow \infty$ and $\frac{c}{a} \rightarrow 0$ ($\Rightarrow \epsilon_i \rightarrow 0 \forall i$) every local deviation from uniformity of \mathcal{P} 's distribution is captured and results in a decrease of $\hat{\chi}$. Finally χ is obtained by normalizing $\hat{\chi}$ by its expected value in the case that P_1, \dots, P_a are picked independently from the uniform distribution:

$$\chi := \frac{\sum_{i=1}^b p(k_i)}{b \sum_{j=0}^a p(j)^2} = \frac{\sum_{i=1}^b \tilde{p}(k_i) \sum_{j=0}^a \tilde{p}(j)}{b \sum_{j=0}^a \tilde{p}(j)^2}.$$

-
- [1] S. H. Strogatz, *Nature* **410**, 268 (2001).
 - [2] R. Albert and A.-L. Barabási, *Rev. Mod. Phys.* **74**, 47 (2002).
 - [3] M. E. J. Newman, *SIAM Rev.* **45**, 167 (2003).
 - [4] S. Boccaletti, V. Latora, Y. Moreno, M. Chavez, and D.-U. Hwang, *Phys. Rep.* **424**, 175 (2006).
 - [5] O. Sporns and C. J. Honey, *Proc. Natl. Acad. Sci. U.S.A.* **103**, 19219 (2006).
 - [6] A. Barrat, M. Barthélemy, and A. Vespignani, *Dynamical Processes on Complex Networks* (Cambridge University Press, New York, USA, 2008).
 - [7] J. C. Reijneveld, S. C. Ponten, H. W. Berendse, and C. J. Stam, *Clin. Neurophysiol.* **118**, 2317 (2007).
 - [8] A. Arenas, A. Díaz-Guilera, J. Kurths, Y. Moreno, and C. Zhou, *Phys. Rep.* **469**, 93 (2008).
 - [9] E. Bullmore and O. Sporns, *Nat. Rev. Neurosci.* **10**, 186 (2009).
 - [10] J. F. Donges, Y. Zou, N. Marwan, and J. Kurths, *Europhys. Lett.* **87**, 48007 (2009).
 - [11] A. A. Tsonis, G. Wang, K. L. Swanson, F. A. Rodrigues, and L. da Fontoura Costa, *Clim. Dynam. in press* (2010), 10.1007/s00382-010-0874-3.
 - [12] T. Qiu, B. Zheng, and G. Chen, *New J. Physics* **12**, 043057 (2010).
 - [13] S. H. Yook, H. Jeong, A.-L. Barabási, and Y. Tu, *Phys. Rev. Lett.* **86**, 5835 (2001).
 - [14] A. Barrat, M. Barthélemy, R. Pastor-Satorras, and A. Vespignani, *Proc. Natl. Acad. Sci. U.S.A.* **101**, 3747 (2004).
 - [15] M. E. J. Newman, *Phys. Rev. E* **70**, 056131 (2004).
 - [16] M. Chavez, D.-U. Hwang, A. Amann, H. Hentschel, and S. Boccaletti, *Phys. Rev. Lett.* **94**, 218701 (2005).
 - [17] J. P. Onnela, J. Saramäki, J. Hyvönen, G. Szábo, D. Lazer, K. Kaski, J. Kertész, and A.-L. Barabási, *Proc.*

- Natl. Acad. Sci. U.S.A. **104**, 7332 (2007).
- [18] M. Rubinov, S. A. Knock, C. J. Stam, S. Micheloyannis, A. W. F. Harris, L. M. Williams, and M. Breakspear, *Human Brain Mapp.* **30**, 403 (2009).
- [19] C. J. Stam, W. de Haan, A. Daffertshofer, B. F. Jones, I. Manshanden, A. M. van Cappellen van Walsum, T. Montez, J. P. A. Verbunt, J. C. de Munck, B. W. van Dijk, H. W. Berendse, and P. Scheltens, *Brain* **132**, 213 (2009).
- [20] S. C. Ponten, L. Douw, F. Bartolomei, J. C. Reijneveld, and C. J. Stam, *Exp. Neurol.* **217**, 197 (2009).
- [21] M. Chavez, M. Valencia, V. Navarro, V. Latora, and J. Martinerie, *Phys. Rev. Lett.* **104**, 118701 (2010).
- [22] M.-T. Horstmann, S. Bialonski, N. Noennig, H. Mai, J. Prusseit, J. Wellmer, H. Hinrichs, and K. Lehnertz, *Clin. Neurophysiol.* **121**, 172 (2010).
- [23] L. Wang, C. Yu, H. Chen, W. Qin, Y. He, F. Fan, Y. Zhang, M. Wang, K. Li, Y. Zang, T. S. Woodward, and C. Zhu, *Brain* **133**, 1224 (2010).
- [24] A. S. Pikovsky, M. G. Rosenblum, and J. Kurths, *Synchronization: A universal concept in nonlinear sciences* (Cambridge University Press, Cambridge, UK, 2001).
- [25] E. Pereda, R. Quiñero, and J. Bhattacharya, *Prog. Neurobiol.* **77**, 1 (2005).
- [26] K. Hlaváčková-Schindler, M. Paluš, M. Vejmelka, and J. Bhattacharya, *Phys. Rep.* **441**, 1 (2007).
- [27] K. Lehnertz, S. Bialonski, M.-T. Horstmann, D. Krug, A. Rothkegel, M. Staniek, and T. Wagner, *J. Neurosci. Methods* **183**, 42 (2009).
- [28] C. T. Butts, *Science* **325**, 414 (2009).
- [29] S. Bialonski, M.-T. Horstmann, and K. Lehnertz, *Chaos* **20**, 013134 (2010).
- [30] B. C. M. van Wijk, C. J. Stam, and A. Daffertshofer, *PLoS ONE* **5**, e13701 (2010).
- [31] M. E. J. Newman, S. H. Strogatz, and D. J. Watts, *Phys. Rev. E* **64**, 026118 (2001).
- [32] J. G. Foster, D. V. Foster, P. Grassberger, and M. Paczuski, *Phys. Rev. E* **76**, 046112 (2007).
- [33] D. Garlaschelli and M. I. Loffredo, *Phys. Rev. Lett.* **102**, 038701 (2009).
- [34] S. Maslov and K. Sneppen, *Science* **296**, 910 (2002).
- [35] S. Maslov, K. Sneppen, and A. Zaliznyak, *Physica A* **333**, 529 (2004).
- [36] O. Sporns and J. D. Zwi, *Neuroinformatics* **2**, 145 (2004).
- [37] Y. Artzy-Randrup and L. Stone, *Phys. Rev. E* **72**, 056708 (2005).
- [38] M. Á. Serrano, M. Boguñá, and R. Pastor-Satorras, *Phys. Rev. E* **74**, 055101 (2006).
- [39] M. Á. Serrano, *Phys. Rev. E* **78**, 026101 (2008).
- [40] T. Opsahl, V. Colizza, P. Panzarasa, and J. J. Ramasco, *Phys. Rev. Lett.* **101**, 168702 (2008).
- [41] V. Zlatić, G. Bianconi, A. Díaz-Guilera, D. Garlaschelli, F. Rao, and G. Caldarelli, *Eur. Phys. J. B* **67**, 271 (2009).
- [42] C. I. Del Genio, H. Kim, Z. Toroczkai, and K. E. Bassler, *PLoS ONE* **5**, e10012 (2010).
- [43] J. Theiler, S. Eubank, A. Longtin, B. Galdrikian, and J. D. Farmer, *Physica D* **58**, 77 (1992).
- [44] T. Schreiber and A. Schmitz, *Physica D* **142**, 346 (2000).
- [45] J. P. Onnela, J. Saramäki, J. Kertész, and K. Kaski, *Phys. Rev. E* **71**, 065103 (2005).
- [46] J. Saramäki, M. Kivelä, J. P. Onnela, K. Kaski, and J. Kertész, *Phys. Rev. E* **75**, 027105 (2007).
- [47] M. E. J. Newman, *Phys. Rev. E* **64**, 016132 (2001).
- [48] G. Caldarelli, A. Capocci, P. De Los Rios, and M. A. Muñoz, *Phys. Rev. Lett.* **89**, 258702 (2002).
- [49] A. Barrat, M. Barthélemy, and A. Vespignani, *Phys. Rev. E* **70**, 066149 (2004).
- [50] G. C. Shepard, *Mathematika* **18**, 255 (1971).
- [51] P. A. Rubin, *Commun. Stat. Simulat.* **13**, 375 (1984).
- [52] R. L. Smith, in *Proceedings of the 1996 Winter Simulation Conference*, edited by J. M. Charnes, D. J. Morrice, D. T. Brunner, and J. J. Swain (IEEE Computer Society, Los Alamitos, 1996) pp. 260–264.
- [53] R. L. Smith, *Oper. Res.* **6**, 1296 (1984).
- [54] Fp1, Fp2, F7, F3, Fz, F4, F8, FC1, FC2, T7, C3, Cz, C4, T8, CP1, CP2, P7, P3, Pz, P4, P8, PO7, PO3, PO4, PO8, Oz, O9, Iz, and O10.
- [55] E. Niedermayer and F. H. Lopes da Silva, eds., *Electroencephalography, Basic Principles, Clinical Applications and Related Fields*, 3rd ed. (Williams & Wilkins, Baltimore, 1993).
- [56] F. Mormann, K. Lehnertz, P. David, and C. E. Elger, *Physica D* **144**, 358 (2000).
- [57] K. S. Gleditsch, *J. Conflict Resolut.* **46**, 712 (2002).
- [58] D. Garlaschelli and M. I. Loffredo, *Phys. Rev. Lett.* **93**, 188701 (2004).
- [59] G. Fagiolo, J. Reyes, and S. Schiavo, *Phys. Rev. E* **79**, 036115 (2009).
- [60] G. Fagiolo, J. Reyes, and S. Schiavo, *J. Evol. Econ.* **20**, 479 (2010).
- [61] K. Bhattacharya, G. Mukherjee, J. Saramäki, K. Kaski, and S. S. Manna, *J. Stat. Mech.: Theory Exp.* **2008**, P02002 (2008).
- [62] For the year 1948 we also omitted the Koreas in order to obtain a connected network.